Stable Organic Blue-Light-Emitting Devices Prepared from Poly[spiro(fluorene-9,9′-xanthene)]

Ya-Hsien Tseng, Ping-I Shih, Chen-Han Chien, Ajay Kumar Dixit, and Ching-Fong Shu*

Department of Applied Chemistry, National Chiao Tung University, 300, Hsinchu, Taiwan, R.O.C.

Yi-Hung Liu and Gene-Hsiang Lee

Instrumentation Center, College of Science, National Taiwan University, 107, Taipei, Taiwan, R.O.C.

Received August 15, 2005; Revised Manuscript Received October 5, 2005

ABSTRACT: A short, efficient synthetic route has been developed for the preparation of 2,7-dibromospiro-[fluorene-9,9′-(2′,7′-di-*n*-octyloxyxanthene)], which was subsequently polymerized with the corresponding diborolane through Suzuki coupling to afford a fluorene-based homopolymer, **PSFX**, that contains a spiroxanthene group functionalized on the C-9 position of each fluorene repeat unit. Single-crystal X-ray diffraction analysis of the dibromo monomer revealed that the spiro-fused fluorene and xanthene moieties lie perpendicular to one another. As a consequence of the incorporation of the spiro pendant group, **PSFX** possesses a high glass transition temperature and good thermal stability while displaying its stable blue emission in the solid state. A light-emitting diode device prepared using **PSFX** as the emitting layer exhibits an efficient, stable blue emission; it has a turn-on voltage of 6 V and a maximum external quantum efficiency of 1.74% ph/el. Even when the brightness was increased up to 10^3 cd/m^2 (ca. 11 V), the CIE color coordinates of the resulting EL spectrum remained in the deep-blue region (0.15, 0.07) and the device's efficiency was 1.33% ph/el.

Introduction

Organic electroluminescent materials have recently attracted much interest because of their physical properties and potential applications in light-emitting devices and flat-panel displays.[1,2] In particular, considerable efforts have been made toward the development of new luminescent conjugated polymers. Because they are solution-processable, they may be deposited using conventional low-cost liquid deposition techniques; moreover, their luminescent properties may be fine-tuned through manipulation of their chemical structures. Full-color display applications require that blue-, green-, and red-light-emitting materials be developed that have sufficiently high luminous efficiencies and proper chromaticities. Polyfluorenes (PFs) are very promising candidates for such blue-light-emitting materials because of their high photoluminescence (PL) and electroluminescence (EL) efficiencies, thermal stability, and ready color-tuning through the introduction of low-band-gap comonomers.[3−5] In addition, the facile process of functionalizing the C-9 position of the fluorene unit provides the opportunity to improve both the solubility and processability of the PFs, while also offering the ability to tune their optoelectronic properties.[6,7]

Unfortunately, the tendency to display undesired long-wavelength emission bands upon exposure to heat or during device operation, which results in both color instability and reduced efficiency, has been a crucial problem that has limited the application of polyfluorenes in polymer-based light-emitting diodes (PLEDs). The formation of interchain excimers is believed to be the cause of these long-wavelength emissions.[8] Recently, List et al. claimed that keto defects, which result from the thermo- or photooxidation of the polymers, may also be the source of such low-energy emission bands.[9] Several chemical approaches have been utilized to reduce the formation of excimer or keto defects and to enhance the color stability of polyfluorenes; these approaches include the introduction of low-band-gap chromophores at the end and/or middle of the polymer chain,[10] end-capping with cross-linkable moieties or hole-trapping groups,[11] kinking the backbone structure,[12] encapsulating the polymer backbone within bulky/dendrimer side chains,[13−15] and incorporating siloxane bridges or polyhedral oligomeric silsesquioxane (POSS) units.[16] Among these methods, the introduction of spiro structures is one of the most promising solutions to the problem.[14]

Scheme 1

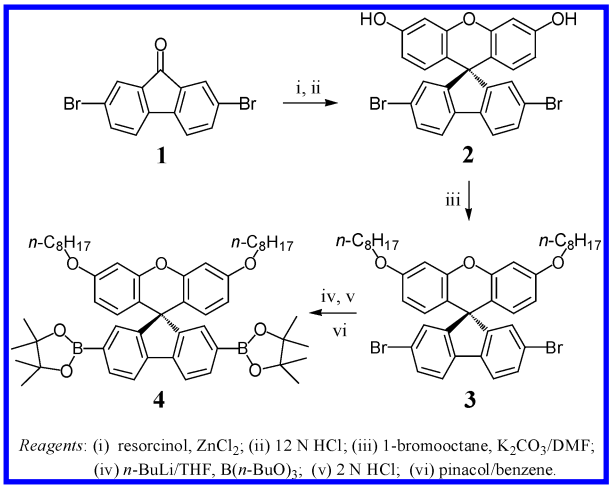

This paper describes the synthesis and characterization of a fluorene-based homopolymer containing a spiro(fluorene-9,9′-xanthene) skeleton. Starting from commercially available 2,7-dibromo-9-fluorenone, a one-step condensation reaction with resorcinol led directly to the spiro(fluorene-9,9′-xanthene) structure and at the same time provided two phenol functionalities for the spiro pendent group,[17] upon which solubilizing side chains could be introduced readily (Scheme 1). Figure

10.1021/ma051798f CCC: $30.25
Published on Web 11/05/2005

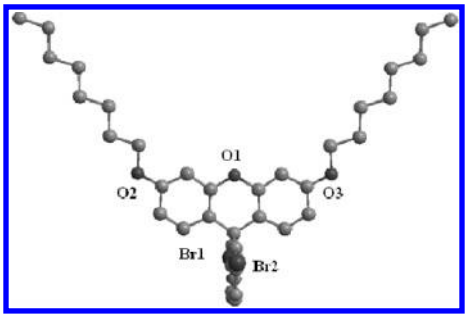

Figure 1. Optimized molecular structure of monomer **3** obtained from AM1 calculations.

1 displays the optimized molecular geometry, obtained by minimizing the energy of AM1 calculations (HyperChem 7.5), of the monomeric fluorene building unit. The fluorene and xanthene moieties are positioned in a nearly planar conformation and are connected through a common tetrasubstituted carbon atom (the spiro center), about which the planes of the two entities are arranged orthogonally (dihedral angle = 89.8°). We anticipated that this three-dimensional structure would restrict close packing of the polymer chains and reduce any interchain $\pi-\pi$ interactions and, consequently, suppress aggregate/excimer formation and enhance PL efficiency. In addition, the C-9 positions of the spiro-structured fluorene units bear only strong $C_{sp^2}-C_{sp^3}$ bonds that are much less susceptible to oxidation;[13b,14e,15a] thus, the problem of ketone defects being induced through oxidative degradation should be overcome.

Experimental Section

Characterization. ^{1}H and ^{13}C NMR spectra were recorded on Varian UNITY INOVA AS500 (500 MHz) and Bruker-DRX 300 (300 MHz) spectrometers. Mass spectra were obtained using a JEOL JMS-HX 110 mass spectrometer. Size exclusion chromatography (SEC) was performed using a Waters chromatography unit interfaced with a Waters 410 differential refractometer; three 5-μm Waters Styragel columns (300 × 7.8 mm) were connected in series in order of decreasing pore size (10^4, 10^3, and 10^2 Å); THF was the eluent. Standard polystyrene samples were used for calibration. Differential scanning calorimetry (DSC) was performed using a SEIKO EXSTAR 6000DSC unit at a heating rate of 20 °C min^{-1} and a cooling rate of 40 °C min^{-1}. Samples were scanned from 30 to 370 °C, cooled to 0 °C, and then scanned again from 30 to 370 °C. The glass transition temperatures (T_g) were determined from the second heating scan. Thermogravimetric analysis (TGA) was undertaken using a Perkin-Elmer TGA Pyris 1 instrument. The thermal stabilities of the samples were determined under nitrogen atmosphere by measuring their weight losses while heating them at a rate of 20 °C min^{-1}. UV−vis spectra were measured using an HP 8453 diode-array spectrophotometer. PL spectra were obtained using a Hitachi F-4500 luminescence spectrometer. Cyclic voltammetry (CV) measurements were performed using a BAS 100 B/W electrochemical analyzer operated at a scan rate of 50 mV s^{-1}; the solvent was anhydrous acetonitrile and 0.1 M tetrabutylammonium hexafluorophosphate ($TBAPF_6$) was the supporting electrolyte. The potentials were measured against an Ag/Ag$^+$ (0.01 M $AgNO_3$) reference electrode; ferrocene was the internal standard.

X-ray Structural Analysis. Single-crystal X-ray diffraction data were obtained using a Bruker Smart ApexCCD diffractometer and λ(Mo Kα) radiation (λ = 0.71073 Å); data collection was executed using the SMART program. Cell refinement and data reduction were undertaken using the SAINT program. The structure was determined using the SHELXTL/PC program and refined using full-matrix least-squares methods.

2,7-Dibromospiro[fluorene-9,9′-(2′,7′-dihydroxyxanthene)] (2). A mixture of 2,7-dibromo-9-fluorenone (**1**, 6.00 g, 17.71 mmol), resorcinol (6.82 g, 62.00 mmol), and $ZnCl_2$ (555 mg, 4.07 mmol) was stirred and heated at 140 °C for 2 h. The melt was then heated with concentrated HCl (aqueous, 20 mL) under reflux for another 1 h. The reaction mixture was poured into water (300 mL). The precipitate was washed with water, dried, and purified by column chromatography (EtOAc/hexane, 1:3) to yield **2** (5.69 g, 61.8%). ^{1}H NMR (acetone-d_6): δ 6.20 (d, J = 8.6 Hz, 2 H), 6.39 (dd, J = 8.6, 2.5 Hz, 2 H), 6.71 (d, J = 2.5 Hz, 2 H), 7.25 (d, J = 1.8 Hz, 2 H), 7.58 (dd, J = 8.1, 1.8 Hz, 2 H), 7.90 (d, J = 8.1 Hz, 2 H), 8.69 (br, 2H). ^{13}C NMR (acetone-d_6): δ 61.2, 104.5, 113.3, 115.4, 123.4, 123.7, 130.0, 130.1, 132.7, 139.3, 153.4, 159.1, 159.3. HREI-MS (m/z): [M]$^+$ calcd for $C_{25}H_{14}O_3{}^{79}Br_2$, 519.9310; found. 519.9310. Anal. Calcd for $C_{25}H_{14}Br_2O_3$: C, 57.50; H, 2.70. Found: C, 57.34; H, 3.28.

2,7-Dibromospiro[fluorene-9,9′-(2′,7′-di-*n*-octyloxyxanthene)] (3). A mixture of **2** (7.80 g, 14.99 mmol), 1-bromooctane (10.42 g, 53.98 mmol), K_2CO_3 (5.38 g, 38.98 mmol), and DMF (132 mL) was stirred and heated at 120 °C for 12 h under N_2. The resulting mixture was poured into water (200 mL) and extracted with EtOAc (3 × 100 mL). The combined extracts were dried ($MgSO_4$), and the solvent was evaporated in vacuo. The crude product was purified by column chromatography (EtOAc/hexane, 1:200) to afford **3** (7.50 g, 67.5%). ^{1}H NMR ($CDCl_3$): δ 0.87 (t, J = 6.1 Hz, 6 H), 1.27−1.43 (m, 20 H), 1.71−1.80 (m, 4 H), 3.92 (t, J = 6.5 Hz, 4 H), 6.23 (d, J = 8.7 Hz, 2 H), 6.38 (dd, J = 8.7, 2.5 Hz, 2 H), 6.71 (d, J = 2.4 Hz, 2 H), 7.21 (d, J = 1.5 Hz, 2 H), 7.45 (dd, J = 8.1, 1.7 Hz, 2 H), 7.58 (d, J = 8.1 Hz, 2 H). ^{13}C NMR ($CDCl_3$): δ 14.1, 22.6, 26.0, 29.15, 29.21, 29.3, 31.8, 53.5, 68.2, 101.8, 111.3, 114.7, 121.3, 122.3, 128.6, 129.0, 131.1, 137.4, 151.9, 157.1, 159.3. HREI-MS (m/z): [M + H]$^+$ calcd for $C_{41}H_{47}O_3{}^{79}Br_2$, 745.1891; found, 745.1891. Anal. Calcd for $C_{41}H_{46}Br_2O_3$: C, 65.96; H, 6.21. Found: C, 66.00; H, 6.17.

2,7-Bis(4,4,5,5-tetramethyl-1,3,2-dioxaborolane-2-yl)-spiro[fluorene-9,9′-(2′,7′-di-*n*-octyloxyxanthene)] (4). *n*-Butyllithium in hexane (2.5 M, 8.31 mL) was added slowly under N_2 to a stirred solution of dibromide **3** (4.00 g, 5.35 mmol) in anhydrous THF (40 mL) at −78 °C. The mixture was warmed to room temperature, stirred for 2 h, and then cooled to −78 °C. Tri-*n*-butyl borate (3.33 mL, 12.3 mmol) was added and then the mixture was warmed slowly to room temperature and stirred for 12 h. Then, 2.0 M HCl (120 mL) was added and the mixture was stirred for 5 h. The reaction mixture was extracted with diethyl ether and the combined organic phases were dried ($MgSO_4$). Concentration under reduced pressure gave the diboronic acid, which, without further purification, was reacted with pinacol (1.36 g, 11.50 mmol) in benzene (12 mL) under reflux for 2 h using a Dean−Stark setup for azeotropic removal of the water that formed. The mixture was concentrated under reduced pressure and the residue was crystallized in hexane to afford **4** (2.19 g, 48.6%). ^{1}H NMR ($CDCl_3$): δ 0.86 (t, J = 6.4 Hz, 6 H), 1.25−1.49 (m, 44 H), 1.69−1.78 (m, 4 H), 3.90 (t, J = 6.5 Hz, 4 H), 6.17 (d, J = 8.7 Hz, 2 H), 6.29 (dd, J = 8.7, 2.4 Hz, 2 H), 6.67 (d, J = 2.4 Hz, 2 H), 7.48 (s, 2 H), 7.77 (d, J = 7.5 Hz, 2 H), 7.80 (d, J = 7.6 Hz, 2 H). ^{13}C NMR ($CDCl_3$): δ 14.1, 22.6, 24.8, 26.0, 29.19, 29.2, 29.3, 31.8, 53.1, 68.1, 83.7, 101.5, 111.0, 115.8, 119.4, 129.3, 131.9, 134.4, 142.2, 151.8, 155.9, 158.7. HRFAB-MS (m/z): [M + H]$^+$ calcd for $C_{53}H_{71}O_7B_2$, 841.5386; found, 841.5387. Anal. Calcd for $C_{53}H_{70}O_7B_2$: C, 75.72; H, 8.39. Found: C, 75.51; H, 8.40.

Poly[2′,7′-di-*n*-octyloxyspiro(fluorene-9,9′-xanthene)-2,7-diyl] (PSFX). Aqueous potassium carbonate (2.0 M, 1.1 mL) and Aliquat 336 (27 mg) were added to a mixture of monomers **3** (88 mg, 118 μmol) and **4** (100 mg, 118 μmol) in distilled toluene (2.2 mL). The mixture was degassed and Pd(PPh_3)$_4$ (ca. 5 mg) was added in one portion under N_2. The solution was then heated at 110 °C for 72 h. The end groups were then capped by heating the mixture under reflux for 12 h with benzeneboronic acid (28 mg, 237 μmol) and then for 12 h with bromobenzene (37 mg, 237 μmol). The reaction mixture was then cooled to room temperature and precipitated into a mixture of MeOH and H_2O [1:1 (v/v), 100 mL]. The crude polymer was collected and washed with excess MeOH. The polymer was dissolved in chlorobenzene and reprecipitated into MeOH before being washed with acetone for 72 h using a

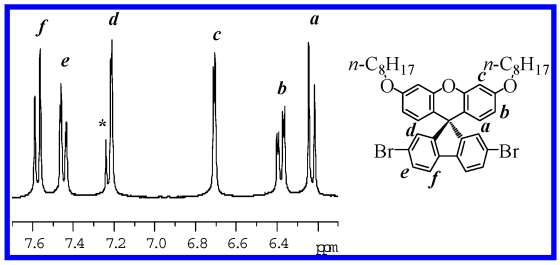

Figure 2. ^{1}H NMR spectrum in the aromatic region of monomer **3** in $CDCl_3$. The asterisk indicates the signal arising from $CHCl_3$.

Soxhlet apparatus. Drying under vacuum gave **PSFX** (120 mg, 95.1%). ^{1}H NMR ($CDCl_3$): δ 0.88 (br, 6 H), 1.29−1.43 (m, 24 H), 1.75 (br, 4 H), 3.92 (br, 4 H), 6.23−6.34 (m, 4 H), 6.64−6.71 (m, 2 H), 7.24−7.36 (m, 2 H), 7.40−7.56 (m, 2 H), 7.66−7.80 (m, 2 H). ^{13}C NMR ($CDCl_3$): δ 14.0, 22.6, 26.1, 29.2, 29.3, 29.4, 31.8, 53.8, 68.3, 102.0, 111.1, 116.7, 120.0, 124.1, 127.0, 128.9, 138.4, 141.2, 152.2, 156.5, 159.1.

Light-Emitting Devices. Polymer LED devices were fabricated in the configuration ITO/poly(styrenesulfonate)-doped poly(3,4-ethylenedioxythiophene) (PEDOT) (35 nm)/light-emitting layer (50−70 nm)/TPBI (30 nm)/Mg:Ag (100 nm)/Ag (100 nm). To improve hole injection and substrate smoothness, the PEDOT was spin-coated directly onto the ITO glass and dried at 80 °C for 12 h under vacuum. The light-emitting layer was spin-coated on top of the PEDOT layer, using toluene as the solvent, and then dried for 3 h at 60 °C under vacuum. Prior to film-casting, the polymer solution was filtered through a Teflon filter (0.45 μm). The TPBI layer, which was grown by thermal sublimation in a vacuum of 3×10^{-6} Torr, was used as an electron-transport layer that blocks holes and confines excitons. The cathode Mg:Ag (10:1, 100 nm) alloy was deposited onto the TPBI layer by coevaporation of the two metals; an additional layer of Ag (100 nm) was deposited onto the alloy as a protection layer. The current−voltage−luminance characteristics were measured under ambient conditions using a Keithley 2400 source meter and a Newport 1835C optical meter equipped with an 818ST silicon photodiode.

Results and Discussion

Synthesis. Scheme 1 illustrates the synthetic route for the preparation of the monomers, each of which contained a spiro(fluorene-9,9′-xanthene) skeleton and two solubilizing alkoxy side chains. The key intermediate—2,7-dibromo-spiro[fluorene-9,9′-(2′,7′-dihydroxyxanthene)] (**2**)—was prepared through a simple acid-catalyzed condensation reaction of 2,7-dibromo-9-fluorenone (**1**) with resorcinol, using $ZnCl_2$/HCl as a condensing agent, to form the spiro framework.[17] Subsequent alkylation of **2** with 1-bromooctane in the presence of K_2CO_3 furnished the dibromo monomer **3** possessing two flexible dialkoxy side chains. Lithiation of **3** using *n*-BuLi, followed by treatment with tri-*n*-butyl borate and hydrolysis in aqueous HCl, gave the corresponding diboronic acid, which, without further purification, was converted to the diborolane monomer **4** through its esterification with pinacol. All of the monomers were characterized using ^{1}H and ^{13}C NMR spectroscopy. In addition to the signals appearing between δ 0.75 and 3.95, which correspond to the resonances of the aliphatic protons of the *n*-octyl chains, the ^{1}H NMR spectrum of **3** exhibits six equally intense signals for the aromatic protons (Figure 2). These aromatic protons were assigned through a detailed analysis of the ^{1}H and ^{13}C NMR data of **3**, aided by such 2D NMR spectroscopy experiments as ^{1}H−^{1}H correlation spectroscopy (^{1}H−^{1}H COSY) and long-range ^{1}H−^{13}C heteronuclear correlation spectroscopy (HMBC). In the ^{13}C NMR spectrum, the signal for a quarternary carbon atom at δ 65.6 (C-9) indicated the presence of the spiro skeleton in **3**. High-resolution mass spectrometric and elemental analysis data provided additional verification of the proposed structures. The molecular structure of monomer **3** was further confirmed by X-ray crystallographic analysis of a single crystal obtained upon slow crystallization of an EtOAc solution of **3**. Figure 3 displays the ORTEP plot of **3** obtained after performing X-ray diffraction at 295 K. The spiro-molecule comprises fluorene and xanthene rings connected through a common tetrahedrally bonded carbon atom (the spiro center). In the spiro-segment, the planes of the fluorene and xanthene units lie almost perpendicular to one another (dihedral angle: 88.2°) in quite good agreement with our calculated structure.

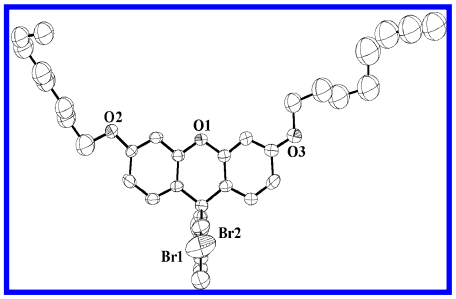

Figure 3. ORTEP diagram of the solid-state structure of monomer **3**; the thermal ellipsoids represent the 30% probability level. Hydrogen atoms have been omitted for clarity.

Scheme 2

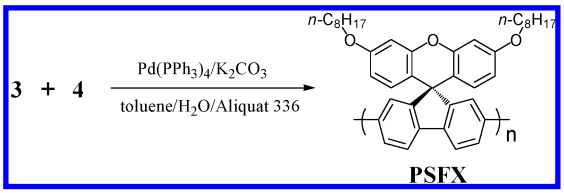

As illustrated in Scheme 2, the spiro-fluorene-based homopolymer poly[2′,7′-di-*n*-octyloxy-spiro(fluorene-9,9′-xanthene)-2,7-diyl] (**PSFX**) was prepared through Suzuki polymerization using equimolar amounts of the dibromide **3** and the diborolane **4**.[18] This polymerization was performed using $Pd(PPh_3)_4$ as the catalyst in a mixture of toluene and aqueous potassium carbonate (2.0 M); Aliquat 336 was added as a phase-transfer reagent. At the end of the polymerization process, the end groups of the polymer chain were capped by heating the reaction mixture under reflux sequentially with phenylboronic acid and bromobenzene, each for a period of 12 h. The resulting polymer solution was precipitated repeatedly into methanol/water and methanol, followed by Soxhlet extraction with acetone to give **PSFX**. The ^{1}H and ^{13}C NMR spectra of **PSFX** are consistent with its expected spiro(fluorene-9,9′-xanthene) structure. The signals between δ 0.75 and 4.10 are assigned to the protons of the *n*-octyloxy chains. The resonances of the aromatic protons of the spiro(fluorene-9,9′-xanthene) repeating units appear between δ 6.15 and 7.92. From auxiliary 2D ^{1}H−^{1}H COSY data, the positions of the chemical shifts of the aromatic protons in **PSFX** were assigned. In the ^{13}C NMR spectrum, the signal of the central spiro carbon atom (C-9) resonates at 68.3 ppm; this value is indicative of the presence of a spiro skeleton in **PSFX**.

PSFX readily dissolves in chlorobenzene and is soluble in chloroform and toluene only upon heating; it has limited solubility in THF. The molecular weight of

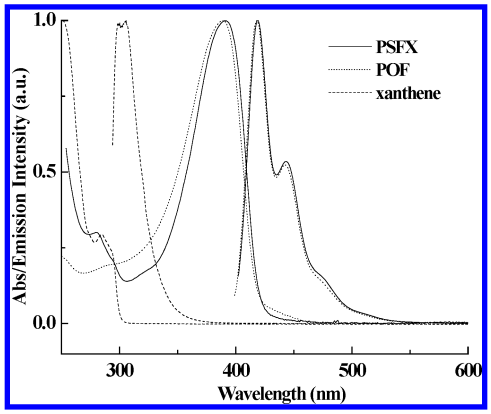

Figure 4. UV−vis absorption and PL spectra of **PSFX**, **POF**, and xanthene, recorded in $CHCl_3$.

Table 1. Photophysical Properties of PSFX, POF, and Xanthene

	solution[a]			film[b]		
	abs (nm)	PL (nm)[c]	Φ_f[d]	abs (nm)	PL (nm)[c]	Φ_f
PSFX	(280) 390	418 (443)	1.00	(281) 393	426 (450)	0.92
POF	389	418 (442)	0.83	390	424 (448)	0.55[e]
xanthene	250 (285)	301				

[a] Evaluated in chloroform. [b] Evaluated in the solid state; prepared from chlorobenzene solutions. [c] Excited at 390 nm. [d] Quantum yield (Φ_f) determined in toluene, relative to 9,10-diphenylanthracence in cyclohexane, upon excitation at 365 nm. [e] The thin film quantum efficiency of POF, as measured in an integrating sphere, was 0.55.[22] [f] Peaks that appear as shoulders or weak bands are provided in parentheses.

this polymer was determined using size exclusion chromatography (SEC; eluent: THF) and calibrating against polystyrene standards. The polymer possesses a number-average molecular weight (M_n) of 1.1×10^4 g/mol and a weight-average molecular weight (M_w) of 1.6×10^4 g/mol. The actual average molecular weights are probably higher than these values, because the polymer was only partially soluble in THF; the insoluble portion may correspond to a higher-molecular-weight material. The thermal properties of **PSFX** were investigated through differential scanning calorimetry (DSC) and thermogravimetric analysis (TGA). The DSC measurements were performed within a temperature range from 30 to 300 °C. A distinct glass transition temperature (T_g) was observed at 149 °C, which is a value that is much higher than that of poly(9,9-dioctylfluorene) (**POF**; T_g = ca. 67 °C).[19] It is evident that replacing the flexible *n*-octyl side chain at the C-9 position of each repeating fluorene unit with a rigid, bulky spiroxanthene pendent group increases the chain rigidity and results in the higher value of T_g. Such a relatively high value of T_g, which could prevent morphological change and suppress the formation of aggregates and excimers upon exposure to heat, is desirable for polymers that are used as emissive materials in light-emitting applications.[20] TGA revealed that **PSFX** exhibits excellent thermal stability; its 5% and 10% weight losses occurred at 411 and 433 °C.

Photophysical Properties. Figure 4 presents the UV−vis absorption and PL spectra of **PSFX** in dilute solutions; Table 1 summarizes the spectral data. For the sake of comparison, Figure 4 also provides the absorption and PL spectra of **POF** and xanthene, which serves as a model compound for studying the optical properties of the pendent groups. In chloroform solution, **PSFX** exhibits two major absorptions: one below 300 nm and the other having its λ_{max} at 390 nm. When compared with the absorption spectra of xanthene and **POF**, the first absorption of **PSFX** (in the short-wavelength region) appears to result from a π-electron transition that occurs predominately from the spiro pendent units; the second signal is assigned to a $\pi-\pi^*$ transition derived from the conjugated polyfluorene backbone. Upon excitation of the polymer main chain at 390 nm, the PL spectrum displays a vibronic fine structure with two sharp emission bands appearing at 418 and 443 nm. The absorption and emission peaks of **PSFX** nearly coincide with those of **POF**; this finding implies that replacing the flexible octyl chains on the repeating fluorene units with rigid spiroxanthene pendent groups does not cause perturbation of the main chain's conjugation. Moreover, upon irradiation at 285 nm—a wavelength in which the absorption of the pendant xanthene unit contributes significantly—the PL spectrum remains identical to that obtained under excitation of the polyfluorene backbone at 390 nm (spectrum not shown); no luminescence from the side chains was detected at ca. 300 nm. This result suggests that efficient Förster energy transfer takes place from the excited higher-energy pendent groups to the lower-energy PF backbone, from which the emission occurs. The PL quantum yield in toluene excited at 365 nm was 1.0, as measured relative to 9,10-diphenylanthrancene (Φ_f = 0.9) as a standard;[21] this value is higher than that measured for **POF** (Φ_f = 0.83).

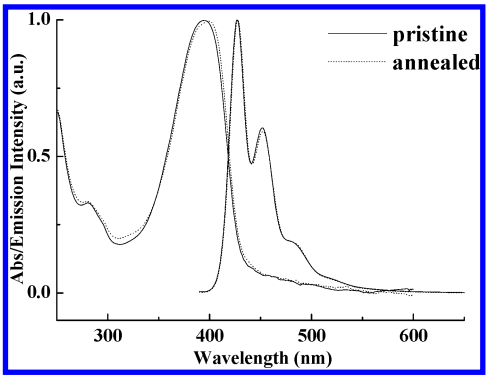

Figure 5. UV−vis absorption and PL spectra of a **PSFX** film before and after annealing it at 150 °C for 20 h under a N_2 atmosphere.

Figure 5 presents the absorption and PL spectra of a **PSFX** film spin-coated from chlorobenzene solution onto a quartz plate. In comparison with the results obtained using dilute solutions, the absorption spectrum of the thin film is slightly broadened, while the emission spectrum displays a red shift of 8 nm. The PL quantum yield of the film was estimated to be 0.92 by comparing its fluorescence intensity with that of the **POF** polymer thin film sample excited at 380 nm (Φ_f = 0.55).[22] The remarkable enhancement in the PL quantum efficiency is probably due to the steric hindrance caused by the spiroxanthene moieties, which prevent interchain $\pi-\pi$ interactions, especially in the solid state; this phenomenon, in turn, reduces the self-quenching that arises from the formation of excimers.[23] The other significant effect of incorporating the pendant spiro unit is the improvement in spectral stability of **PSFX** after thermal treatment. It has been demonstrated that a thin film of **POF** containing flexible alkyl chains exhibits poor spectral stability upon exposure to heat; the cause of this undesirable emissive color instability has been attributed to the formation of aggregates and interchain excimers or to keto defects.[8,9] To examine the effect that

incorporating rigid and bulky spiro pendant groups has on the thermal stability of **PSFX**, the polymer film was heated for 20 h on a hot plate at 150 °C under a N_2 atmosphere and then the absorption and PL spectra were recorded once the films had cooled to room temperature. Figure 5 indicates that both the absorption and PL spectra remained virtually unchanged after such thermal treatment. In addition to the DSC data, this result provides further evidence for the high thermal stability of **PSFX**. In contrast, previous reports indicated that the annealing of a **POF** film resulted not only in a bathochromic shift in the PL wavelength but also in the appearance of an additional emission band between 500 and 600 nm.[14d,24] The enhanced spectral stability of **PSFX** is attributed to the presence of the spiroxanthene pendent groups, which restrict close packing of the polymer chains, reduce the probability of interchain interactions, and, consequently, suppress the tendency of the spiro-polymers to form aggregates and excimers upon thermal treatment. Moreover, the C-9 positions of the substituted fluorene units in the spiroxanthene moieties bear strong C_{sp2}–C_{sp3} bonds, which are quite insusceptible to oxidation;[13b,14e,15a] accordingly, we believe that the ketone defects induced by oxidative degradation are diminished significantly.

Electrochemical Properties. Cyclic voltametry (CV) was employed to investigate the redox behavior of **PSFX** and to estimate its HOMO and LUMO energy levels. The electrochemical behavior of a **PSFX** film coated on a glassy carbon electrode was studied in an electrolyte of 0.1 M tetrabutylammonium hexafluorophosphate ($TBAPF_6$) in acetonitrile; ferrocene was used as the internal standard. From the onset potential of the oxidation process, which was 0.99 V, the HOMO energy level of **PSFX** was estimated to be 5.79 eV with regard to the energy level of ferrocene (4.8 eV below vacuum).[25] This value almost coincides with the HOMO energy level of **POF** ($I_p = 5.8$ eV).[26] The LUMO energy of **PSFX** was estimated by subtraction of the optical band gap energy (E_g) from the HOMO energy. The optical band gap for **PSFX**, taken as the absorption onsets of the UV−vis spectrum of the polymer film, was found to be $E_g = 2.92$ eV; this value led to an estimated value of 2.87 eV for the LUMO energy level (cf. 2.85 eV for **POF**).[26] The similarities in the HOMO and LUMO energy levels of **PSFX** and **POF** indicate that the incorporation of spiroxanthene pendent groups does not affect the redox properties of the fluorene polymer.

Electroluminescence Properties of the LED Device. To evaluate the potential for using **PSFX** as a blue-light-emitting material in polymer LED applications, an EL device was fabricated in the configuration ITO/PEDOT (35 nm)/**PSFX** (50−70 nm)/TPBI (30 nm)/Mg:Ag (100 nm)/Ag(100 nm). The PEDOT layer was used both to facilitate hole injection and to smooth out the surface of the ITO layer; the TPBI layer, which was deposited by thermoevaporation, was employed to transport electrons and block holes. Figure 6 indicates that this device emitted a deep-blue color—two sharp bands appear at 428 and 454 nm in the EL spectrum—corresponding to CIE color coordinates of (0.15, 0.06) at 7 V. The EL spectrum is nearly identical—with respective to position and shape—to the PL spectrum described above; this finding indicates that both the PL and EL originate from the same radiative decay process of the singlet exciton. It has been reported that, during device operation, devices incorporating polydialkylfluorene as the active layer exhibit an undesirable low-energy emission band (between 500 and 600 nm), which turns the pure-blue emission into a blue-green color, i.e., the emission color is unstable.[9] In contrast, the **PSFX**-based device exhibits a voltage-independent and stable EL spectrum. Upon increasing the applied voltage from 7 to 11 V (i.e., near the voltage required to achieve maximum brightness), we observed no significant change in the appearance of the EL spectra. While the voltage was increased up to 13 V, i.e., a potential that exceeded the voltage required for maximum brightness, the EL spectrum became broad in the long wavelength region and a shoulder at ca. 530 nm began to appear, probably as a result of the formation of fluorenone defects.[9] Figure 7 displays the current−voltage ($I-V$) and luminance−voltage ($L-V$) characteristics of the device that was turned on at 6 V (corresponding to 1 cd/m^2); the maximum external quantum efficiency was 1.74% ph/el. Even when the brightness was increased up to 10^3 cd/m^2 (ca. 11 V), the CIE color coordinates of the resulting EL spectrum remained in the deep-blue region (0.15, 0.07) and the device efficiency was 1.33% ph/el (0.82 cd/A). These results clearly demonstrate that **PSFX** is a promising material for creating stable blue emissions in PLEDs. Further improvements in the EL performance may be possible upon optimizing the device structure.

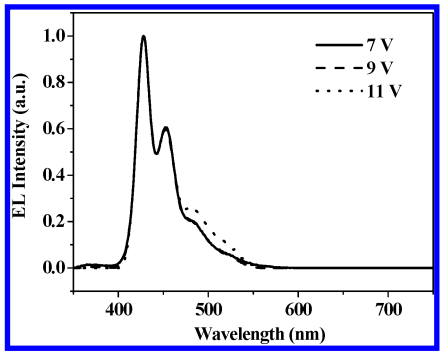

Figure 6. EL spectra of the ITO/PEDOT/**PSFX**/TPBI/Mg:Ag/Ag device recorded at various voltages.

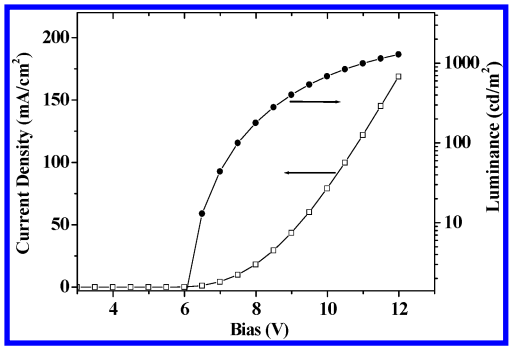

Figure 7. Current density−voltage−luminance characteristics of the **PSFX**-based device.

In conclusion, a facile synthetic route has been developed for the preparation of a fluorene-based homopolymer, **PSFX**, which contains a spiroxanthene group functionalized on the C-9 position of each fluorene repeating unit. In the spiro(fluorene-xanthene) configuration, the fluorene and xanthene moieties are positioned nearly planar and are connected orthogonally through a common tetrasubstituted carbon atom. Because of this rigid 3-D structure, **PSFX** possesses a high value of T_g and very good thermal stability. In addition, the polymer exhibits stable blue PL and EL emission,

unlike those of previous dialkylfluorene-based polymers. This feature allows the preparation of efficient, stable, blue-light-emitting PLEDs when using **PSFX** as the emitting layer.

Acknowledgment. The authors thank the National Science Council for financial support. Special thanks go to Professor C.-H. Cheng for his support during the preparation and characterization of the light-emitting devices.

Supporting Information Available: Figures showing ^{1}H and 2D (^{1}H−^{1}H COSY and HMBC) NMR spectra of monomer **3** and a DSC thermogram of **PSFX**, and an X-ray crystallographic file (CIF) for monomer **3**. This material is available free of charge via the Internet at http://pubs.acs.org.

References and Notes

(1) Mitschke, U.; Bäurele, P. *J. Mater. Chem.* **2000**, *10*, 1471.
(2) (a) Kraft, A.; Grimsdale, A. C.; Holmes, A. B. *Angew. Chem., Int. Ed.* **1998**, *37*, 402. (b) Friend, R. H.; Gymer, R. W.; Holmes, A. B.; Burroughes, J. H.; Marks, R. N.; Taliani, C.; Bradley, D. D. C.; Dos Santos, D. A.; Brédas, J. L.; Lögdlund, M.; Salaneck, W. R. *Nature (London)* **1999**, *397,* 121. (c) Bernius, M. T.; Inbasekaran, M.; O'Brien, J.; Wu, W. *Adv. Mater.* **2000**, *12*, 1737.
(3) (a) Pei, Q.; Yang, Y. *J. Am. Chem. Soc.* **1996**, *118*, 7416. (b) Leclerc, M. *J. Polym. Sci., Part A: Polym. Chem.* **2001**, *39*, 2867. (c) Neher, D. *Macromol. Rapid Commun.* **2001**, *22*, 1365. (d) Becker, S.; Ego, C.; Grimsdale, A. C.; List, E. J. W.; Marsitzky, D.; Pogantsch, A.; Setayesh, S.; Leising, G.; Müllen, K. *Synth. Met.* **2002**, *125*, 73.
(4) (a) Liu, B.; Yu, W. L.; Lai, Y. H.; Huang, W. *Chem. Mater.* **2001**, *13*, 1984. (b) Beaupré, S.; Leclerc, M. *Adv. Funct. Mater.* **2002**, *12*, 192. (c) Herguth, P.; Jiang, X.; Liu, M. S.; Jen, A. K.-Y. *Macromolecules* **2002**, *35*, 6094. (d) Liu, M. S.; Luo, J. Jen, A. K.-J. *Chem. Mater.* **2003**, *15*, 3496. (e) Yang, R.; Tian, R.; Yang, Y.; Hou, Q.; Cao, Y. *Macromolecules* **2003**, *36*, 7453. (f) Niu, Y.-H.; Hou, Q.; Cao, Y. *Appl. Phys. Lett.* **2003**, *82*, 2163. (g) Niu, Y.-H.; Huang, J.; Cao, Y. *Adv. Mater.* **2003**, *15*, 807. (h) Müller, C. D.; Falcou, A.; Reckefuss, N.; Rojahn, M.; Wiederhirn, V.; Rudati, P.; Frohne, H.; Nuyken, O.; Becker, H.; Meerholz, K. *Nature (London)* **2003**, *421*, 829. (i) Yang, J.; Jiang, C.; Zhang, Y.; Yang, R.; Yang, W.; Hou, Q.; Cao, Y. *Macromolecules* **2004**, *37*, 1211. (j) Yang, R.; Tian, R.; Yan, J.; Zhang, Y.; Yang, J.; Hou, Q.; Yang, W.; Zhang, C.; Cao, Y. *Macromolecules* **2005**, *38*, 244.
(5) (a) Ego, C.; Marsitzky, D.; Becker, S.; Zhang, J.; Grimsdale, A. C.; Müllen, K.; MacKenzie, J. D.; Silva, C.; Friend, R. H. *J. Am. Chem. Soc.* **2003**, *125*, 437. (b) Su, H.-J.; Wu, F.-I.; Shu, C.-F. *Macromolecules*, **2004**, *37*, 7197. (c) Su, H.-J.; Wu, F.-I.; Tseng, Y.-H.; Shu, C.-F. *Adv. Funct.* Mater. **2005**, *15*, 1209.
(6) (a) Ego, C.; Grimsdale, A. C.; Uckert, F.; Yu, G.; Srdanov, G.; Müllen, K. *Adv. Mater.* **2002**, *14*, 809. (b) Pogantsch, A.; Wenzl, F. P.; List, E. J. W.; Leising, G.; Grimsdale, A. C.; Müllen, K. *Adv. Mater.* **2002**, *14*, 1061.
(7) (a) Wu, F.-I.; Reddy, D. S.; Shu, C.-F.; Liu, M. S.; Jen, A. K.-Y. *Chem. Mater.* **2003**, *15*, 269. (b) Shu, C.-F.; Dodda, R.; Wu, F.-I.; Liu, M. S.; Jen, A. K.-Y. *Macromolecules* **2003**, *36, 6698.*
(8) (a) Lee, J. I.; Klaerner, G.; Miller, R. D. *Synth. Met.* **1999**, *101*, 126. *(b)* Lee, J. I.; Klarner, G.; Miller, R. D. *Chem. Mater.* **1999**, *11*, 1083. (c) Zeng, G.; Yu, W. L.; Chua, S. J.; Huang, W. *Macromolecules* **2002**, *35*, 6907.
(9) (a) Scherf, U.; List, E. J. W. *Adv. Mater.* **2002**, *14*, 477. (b) List, E. J. W.; Gunter, R.; Scandiucci de Freitas, P.; Scherf, U. *Adv. Mater.* **2002**, *14*, 374. (c) Gaal, M.; List, E. J. W.; Scherf, U. *Macromolecules* **2003**, *36*, 4236. (d) Gong, X.; Iyer, P. K.; Moses, D.; Bazan, G. C.; Heeger, A. J.; Xiao, S. S. *Adv. Funct. Mater.* **2003**, *13*, 325. (e) Kulkarni, A. P.; Kong, X.; Jenekhe, S. A. *J. Phys. Chem. B*. **2004**, 108, 8689.
(10) (a) Kreyenschmidt, M.; Klaemer, G.; Fuhrer, T.; Ashenhurst, J.; Karg, S.; Chen, W. D.; Lee, V. Y.; Scott, J. C.; Miller, R. D. *Macromolecules* **1998**, *31*, 1099. (b) Klärmer, G.; Davey, M. H.; Chen, W. D.; Scott, J. C.; Miller, R. D. *Adv. Mater.* **1998**, *10*, 993. (c) Klärmer, G.; Davey, M. H.; Lee, J.-I.; Miller, R. D. *Adv. Mater.* **1999**, *11*, 115. (d) Lee, J. I.; Hwang, D. H.; Park, H.; Do, L. M.; Chu, H. Y.; Zyung, T.; Miller, R. D. *Synth. Met.* **2000,** *111*, 195.
(11) (a) Klärmer, G.; Lee, J.-I.; Lee, V. Y.; Chan, E.; Chen, J.-P.; Nelson, A.; Markiewicz, D.; Siemens, R.; Scott, J. C.; Miller, R. D. *Chem. Mater.* **1999**, *11*, 1800. (b) Miteva, T.; Meisel, A.; Knoll, W.; Nothofer, H. G.; Scherf, U.; Müller, D. C.; Meerholz, K.; Yasuda, A.; Neher, D. *Adv. Mater.* **2001**, *13*, 565.
(12) Xia, C.; Advincula, R. C. *Macromolecules* **2001**, *34*, 5854.
(13) (a) Lee, J.-H.; Hwang, D.-H. *Chem. Commun.* **2003**, 2836. (b) Jacob, J.; Zhang, J.; Grimsdale, A. C.; Müllen, K.; Gaal, M.; List, E. J. W.; *Macromolecules* **2003**, *36*, 8240.
(14) (a) Yu, W.-L.; Pei, J.; Huang, W.; Heeger, A. J. *Adv. Mater.* **2000**, *12*, 828. (b) Lee, J.-I.; Lee, H.; Oh, J.; Chu, H. Y.; Kim, S. H.; Yang, Y. S.; Kim, G. H.; Do, L.-M.; Zyung, T. *Curr. Appl. Phys.* **2003**, *3*, 469. (c) Wu, Y.; Li, J.; Fu, Y.; Bo, Z. *Org. Lett.* **2004**, *6*, 3485. (d) Wu, F.-I.; Dodda, R.; Jakka, K.; Huang, J.-H.; Hsu C.-S.; Shu, C.-F. *Polymer* **2004**, *45*, 4257. (e) Vak, D.; Chun, C.; Lee, C. L.; Kim, J.-J.; Kim, D.-Y. *J. Mater. Chem.* **2004**, *14*, 1342. (f) Vak, D.; Shin, S. J.; Yum, H.-H.; Kim, S.-S.; Kim, D.-Y. *J. Lumin.* **2005**, *115*, 109.
(15) (a) Setayesh, S.; Grimsdale, A. C.; Weil, T.; Enkelmann, V.; Müllen, K.; Meghdadi, F.; List, E. J. W.; Leising, G. *J. Am. Chem. Soc.* **2001**, *123*, 946. (b) Marsitzky, D.; Vestberg, R.; Blainey, P.; Tang, B. T.; Hawker, C. J.; Carter, K. R. *J. Am. Chem. Soc.* **2001**, *123*, 6965. (c) Tang, H.-Z.; Fujiki, M.; Zhang, Z.-B.; Torimitsu, K.; Motonaga, M. *Chem. Commun.* **2001**, 2426. (d) Chou, C.-H.; Shu, C.-F. *Macromolecules* **2002**, *35*, 9673.
(16) (a) Xiao, S.; Nguyen, M.; Gong, X.; Cao, Y.; Wu, H.; Moses, D.; Heeger, A. J. *Adv. Funct. Mater.* **2003**, *13*, 25. (b) Cho, H.-J.; Jung, B.-J.; Cho, N. S.; Lee, J.; Shim, H.-K. *Macromolecules* **2003**, *36*, 6704. (c) Lin, W. J.; Chen, W. C.; Wu, W. C.; Niu, Y. H.; Jen, A. K. Y. *Macromolecules* **2004**, *37*, 2335. (d) Lee, J.; Cho, H.-J.; Jung, B.-J.; Cho, N. S.; Shim, H.-K. *Macromolecules* **2004**, *37*, 8523. (e) Chou, C.-H.; Hsu, S.-L.; Dinakaran, K.; Chiu, M.-Y.; Wei, K.-H. *Macromolecules* **2005**, *38*, 745.
(17) Bischoff, F.; Adkins, H. *J. Am. Chem. Soc.* **1923**, *45*, 1030.
(18) Miyaura, N.; Suzuki, A. *Chem. Rev.* **1995**, *95*, 2457.
(19) Kulkarni, A. P.; Zhu, Y.; Jenekhe, S. A. *Macromolecules* **2005**, *38*, 1553.
(20) Tokito, S.; Tanaka, H.; Noda, K.; Okada, A.; Taga, Y. *Appl. Phys. Lett.* **1997**, *70*, 1929.
(21) Eaton, D. *Pure Appl. Chem.* **1998**, *60*, 1107.
(22) Grice, A. W.; Bradley, D. D. C.; Bernius, M. T.; Inbasekaran, M.; Wu, W. W.; Woo, E. P. *Appl. Phys. Lett.* **1998**, *73*, 629.
(23) (a) Jenekhe, S. A.; Osaheni, J. A. *Science* **1994**, *265*, 765. (b) Cornil, J.; dos Santos, D. A.; Crispin, X.; Silbey, R.; Bredas, J. L. *J. Am. Chem. Soc.* **1998**, *120*, 1289.
(24) Kulkarni, A. P.; Jenekhe, S. A. *Macromolecules* **2003**, *36*, 5285.
(25) Pommerehne, J.; Vestweber, H.; Guss, W.; Mahrt, R. F.; Bässler, H.; Porsch, M.; Daub, J. *Adv. Mater.* **1995**, *7*, 551.
(26) Janietz, S.; Bradley, D. D. C.; Grell, M.; Giebeler, C.; Inbasekaran, M.; Woo, E. P. *Appl. Phys. Lett.* **1998**, *73*, 2453.

MA051798F